LAWRENCE
LIVERMORE
NATIONAL
LABORATORY

LLNL-JRNL-691078

Shape dependence of laser-particle interaction induced damage on the protective capping layer of 1 high reflector mirror coatings

S. R. Qiu, M. A. Norton, J. Honig, A. M. Rubenchik, C. D. Boley, A. Rigatti, C. J. Stolz, M. J. Matthews

May 5, 2016

Journal of Optical Engineering

Disclaimer

Shape dependence of laser-particle interaction induced damage on the protective capping layer of 1ω high reflector mirror coatings

S.R. Qiu[a,*], M.A. Norton[a], J. Honig[a], A.M. Rubenchik[a], C.D. Boley[a], A. Rigatti[b], C.J. Stolz[a], and M.J. Matthews[b]

[a]Lawrence Livermore National Laboratory, 7000 East Avenue, Livermore, CA 94551

[b]Laboratory for Laser Energetics, University of Rochester, 250 E. River Rd., Rochester NY 14623

Abstract. The response of a potential candidate protective capping layer (SiO_2 or Al_2O_3) to laser exposure of 1ω (1053 nm) to high-reflector silica-hafnia multilayer coatings, in the presence of variously shaped Ti particles is investigated by combining laser damage testing and numerical modeling. Each sample is exposed to a single oblique angle (45°) laser shot (p-polarization, ~ 10 J/cm^2, 14 ns), in the presence of spherically or irregularly shaped Ti particles on the surface. The two capping layers show markedly different responses. For the spherical particles, the Al_2O_3 cap layer exhibits severe damage, with the capping layer becoming completely delaminated at the particle locations. The SiO_2 capping layer is only mildly modified by a shallow depression, likely due to plasma erosion. The different response of the capping layer is attributed to the large difference in thermal expansion coefficient of the materials, with that of the Al_2O_3 about 15 times greater than that of the SiO_2 layer. For the irregular particles, the Al_2O_3 capping layer displays minimal to no damage while the SiO_2 capping layer is significantly damaged. The difference is due to the disparity in mechanical strength with Al_2O_3 possessing approximately 10 times higher fracture toughness.

Key words: Protective coating layer, Contamination, High reflector, Multilayer coatings, Laser damage, Plasmas, 1ω, 1053 nm, High peak power laser.

*Corresponding author: qiu2@llnl.gov, Phone: (925) 422-1636 Fax: (925) 423-0792

1. Introduction

The performance of multilayer dielectric (MLD) coatings of high reflector mirrors in high-peak-power laser systems, including the National Ignition Facility (NIF), Laser Megajoule, and OMEGA [1-3] can be limited by surface contamination. While handling and processing may contribute to unwanted particulate generation, the major contamination sources are derived from components that surround the mirrors within the laser system [4-6], such as beam dumps and fasteners. Typical contaminants that have been found include both organic and inorganic materials, such as oil, polyester fibers, ceramics, metals and metal oxides. In addition to having a large range of chemical composition, contaminants also have a variety of morphologies including spherical, disc-like, or irregular shape.

For highly reflective MLD coatings, adding an absentee overcoat or protective capping layer above the outermost layer has been shown to increase the resistance to laser-induced damage [7-9]. A similar strategy of adding a protective capping layer has also been adopted to extend the lifetime of multilayer mirrors in extreme ultraviolet lithography applications [10]. However, the underlying mechanism by which the coupling between the laser and contaminant causes damage to the protective layer is still elusive. In order to facilitate effective selection and design of capping materials and to develop a practical solution for contaminant removal and post mitigation [11, 12], an improved understanding of the physical principles is desirable.

An early study showed that the laser-induced damage to the reflective surface is strongly dependent on the contaminant composition and size, as well as the laser fluence [13]. In the present work, we extend that study to explore how the laser-induced damage depends on the contaminant shape. We use Ti particles, a common surface contaminant found on MLD mirrors presiding in close proximity to Ti-based beam dumps in high energy laser systems. One selected

shape is spherical, and another shape is irregular (sickle-shaped). To account for the role of the highly reflective surface, we utilize an oblique angle of incidence of the laser beam to reveal the impact of field intensification from multiple reflections between the MLD coating surfaces and the surface of the particle. Specifically, in the given geometry, we investigate the response of the capping layer under 45° oblique irradiation of a single pulse of laser light (1053 nm, p-polarized, fluence ~10 J/cm^2, pulse length 14 ns), in the presence of both spherically- and irregularly-shaped Ti particles. The high reflector (>99.5% HR) samples were silica-hafnia multilayer coatings fabricated by e-beam physical vapor deposition (e-PVD). Silica-hafnia multilayers are commonly used for high reflectors in high peak-power laser systems which require high laser damage resistance [14, 15]. The capping layer materials used in this study are amorphous Al_2O_3 and the previously used SiO_2 [8], respectively. Al_2O_3 is a large bandgap material with a large thermal expansion coefficient (8 ppm/K) and high mechanical strength and has been shown to have high laser-damage resistance [16-18]. Recent studies have demonstrated that this material can be successfully integrated with silica-hafnia multilayer coatings by e-PVD for large-aperture high-fluence laser systems [15].

We find that under similar exposure conditions, the response of the capping layer to laser-particle interaction demonstrates great contrast and is strongly dependent on the Ti particle shape. As shown in our previous work [19], for a spherically-shaped Ti particle, the laser induced damage is more pronounced on the Al_2O_3 capping surface than on the SiO_2 capping surface. The observed difference is attributed to heating of the substrate by the ablated plasma and the large disparity in the thermal expansion coefficients of the two capping materials, with that of the Al_2O_3 layer being about 15 times greater than that of SiO_2 [19]. On the other hand, for irregularly-shaped Ti particles as investigated in the current work, plasma mainly ablates

outward, producing recoil momentum, and the laser-induced damage is more severe on the SiO_2 surface than on the Al_2O_3 layer. This difference is related to the large difference in mechanical toughness between the two materials, with that of Al_2O_3 much greater than that of the SiO_2. Our findings provide fundamental criteria for the selection of high laser damage resistance materials for different applications.

2. Experimental Method

2.1 Coating Sample Preparation

The high reflector (>99.5% R) coatings were designed for a 1053 nm center wavelength, 45° angle of incidence, and p-polarization application. The design utilized 35 quarter-wave layers of alternating hafnia and silica with a half-wave top capping layer of either Al_2O_3 (thickness: 360 nm) or SiO_2 (thickness: 410 nm). The multilayer high reflector samples with different capping layer compositions were fabricated through physical vapor deposition in a 54-in. or a 56-in. vacuum chamber equipped with quartz heater lamps, dual electron-beam guns, multi-point quartz crystal monitors, a planetary substrate rotation, and cryopumps. Granular SiO_2 was evaporated from a continuously rotating pan while Hf metal or Al_2O_3 granules were deposited from a stationary six-pocket electron-beam gun [20]. The chamber was back-filled with oxygen during deposition of the Hf layers in order to oxidize the vapor plume at the substrate, resulting in a thin film coating of HfO_2. The oxygen back-fill for the SiO_2 and Al_2O_3 layers was optimized for thin film stress control while simultaneous not significantly impacting the deposited material stoichiometry [15, 21].

2.2 Laser damage testing

The laser system used for these tests was a Nd: glass zig-zag slab amplifier phase-conjugated laser system capable of producing a 25 J, 1053 nm wavelength, 14 ns FWHM pulses of near diffraction-limited beam quality, single shot to 2 Hz. All fluence values, as measured with a calibrated scientific grade camera at the plane of the sample, are reported normal to the propagation direction. Typical contrast as imaged at the sample plane was ~26% in the central 70% of the approximately 6 x 6 mm^2 square beam. The actual beam area on the substrate was ~0.5 cm^2 due to the 45° angle of incidence. The peak fluence within the beam was typically two times the average fluence. The repetition rate of the laser used during these tests was 0.3 Hz. An additional camera was used with the reflected light to image the surface and obtain the location of the particles in the beam. An online, long-working-distance microscope was the 3rd camera used during laser irradiation. It had sufficient resolution to observe the plasma generated during a laser shot. For the experiments reported here, the 3rd camera was primarily used to identify possible damage during the conditioning shots prior to Ti particle application. A similar setup of the laser system is described in detail in [13].

Prior to contaminant-induced laser damage testing, the surface of each sample of capping layer materials was first laser-conditioned by increasing the fluence from 1 J/cm^2 to 15 J/cm^2 in steps of 0.2 J/cm^2 (1053 nm, 14 ns). Laser-conditioned surfaces were then contaminated with evenly distributed Ti particles of either spherical shape or irregular-shaped filings, which were sprinkled onto the test area by tapping a sheet of paper containing a layer of the particles approximately 30 cm above the sample. The Ti spheres were purchased commercially (Goodfellow, USA) and the filings were home-made by filing a high purity Ti plate. Prior to application to the sample surface, the fabricated filings were separated by size using particle sieves in 100 micron increments. The spheres had a nominal 30 ± 16 μm diameter, and the filings had an average

length of 150 μm and a width of 40-55 μm. Each sample was placed vertically in the testing system with a beam incident angle of 45°.

For the damage initiation study, the surfaces, with the deposited Ti particles, were exposed to a single shot of the laser pulse (p-polarized, 1053 nm, 14 ns) at a fluence of 10 ± 6 J/cm^2. The sample surface under laser irradiation was monitored in real time by an online microscope camera (with resolution ~12 microns per pixel).

2.3 Optical Modeling

The fluence at the particle surface cannot be inferred immediately from the incident laser fluence, due to the important role of the light reflected from the mirror and interfering at the particle-MLD interface. Since the size of the Ti particles is much larger than the laser wavelength, ray tracing is suitable for optical modeling. Interference effects are expected to be significant only in the vicinity of the point of contact with the mirror, where the intensity is low. In fact, electromagnetic theory-based calculations using a finite-difference time-domain (FDTD) method in two dimensions show that the contribution of interference to the absorption power of the Ti particle at the length scales studied is insignificant [19]. To carry out the ray tracing, we employed the commercial application FRED (distributed by Photon Engineering, LLC, Tucson, Arizona), a multipurpose optics code widely used in optical design and analysis. We previously used this code in calculating laser interactions with composite materials [22] and metal powders [23]. Each ray travels from surface to surface, with a particular power in each polarization. At the surface of the particle, rays are absorbed and reflected according to the Fresnel absorptivity and reflectivity of Ti (index of refraction taken as n =3.45 + 4i). The absorbed power is recorded, and only the reflected ray is followed. The absorptivity and reflectivity depend on both the angle of incidence and the polarization.

2.4 Optical and Electron Microscopy

Laser-exposed samples were characterized by a high resolution scanning optical microscope (~0.9 μm/pixel, Benchmark, View MicroMetrology) for particle distribution, damage morphology and topology, respectively. Analysis of images from both online and offline microscopes also led to the assessment of the evolution of the damage size in terms of the number of laser shots and to the calculation of damage growth coefficient of coatings with different capping layer composition due to the laser-Ti particle interaction.

3. Results

The typical morphologies of Ti particles used for the current study are shown in Fig. 1. While the commercially available Ti particles are all smooth surface spheres (Fig. 1a), the homemade filings exhibit irregular, mostly sickle-shaped morphologies with relatively rough surfaces (Fig. 1b). The sprinkled Ti spherical particles on the Al_2O_3 capping layer surface are shown in Fig. 2a. While variations in size are inevitable, the majority of the particles on the surface were approximately 30 μm in diameter. The apparently larger particles were usually aggregates of smaller ones. Exposure to a single shot laser at 45° off normal with an average fluence of 10 J/cm^2 leads to damage on the capping surface which is characterized by the distorted oval features (light areas) in Fig. 2b. It is noted that part of the results from the spherical Ti particle-induced-damage on capping layers have been discussed in detail in Ref. [19]. For the purpose of clear comparison of results obtained from different Ti particle shape, relevant results from the previous work with Ti spherical particles are adopted in the current presentation (Figs. 2b and 4b).

A comparison of Fig. 2a to Fig. 2b shows that nearly all of the damage sites are at the locations of a Ti particle. However, some damage sites appear at locations where no Ti particles are found, suggesting that some particles were relocated during transportation of the test sample between microscope imaging and laser damage testing. However, no original particles were observed after the laser shot. The size of these damage sites ranged from a few μm to approximately 400 μm along the longer dimension. The damage sites had an approximate depth relative to the pristine top layer ranging between 250 nm and 350 nm consistent with previous observations [19]. Since the capping layer was ~360 nm thick, the result suggests that damage was caused by a partial to full removal of the capping materials at the damage sites.

The distribution of Ti spheres on the SiO_2 capping layer surface (Fig. 3a) was similar to that on the Al_2O_3 capping layer surface. The surface was also modified at the locations of a Ti particle after one laser shot of identical conditions (Fig. 3b). However, the change in the capping layer is drastically different from that observed on the Al_2O_3 surface shown in Fig. 2b. Significantly, there is no surface layer delamination. Instead the modified sites all show an apparent depression or erosion from the original surface with the depth of approximately 150 nm [19]. Similar plasma-etched pits have been reported for both input and exit surface fused silica surfaces with metal contaminants under pulsed laser exposures [24, 25]. On both capping layers, associated with the surface modification, there are trails of Ti droplets appearing along the beam direction in the vicinity of the damage.

The response of the two capping layers to the laser-Ti irregular particle interaction is opposite to that of the laser-Ti spherical particle interaction. With Ti filing particles, the laser interaction-induced damage is more pronounced on SiO_2 than on Al_2O_3. Fig. 4a shows the surface of the

Al_2O_3 capping layer after the laser exposure. At the Ti filing location, there is essentially no surface modification except one as indicated by the arrow in Fig. 4a. Instead, the surface contains fragmented Ti particles near the original Ti particle locations. The shape of the resulting fragments (the dark spots in the image) resembles the original sickle shape of the Ti filings. Fig. 4b shows the surface of the SiO_2 capping layer after the laser exposure. Near the original particle location, fragmented Ti particles (from sub-microns to a few microns) are observed. Interestingly, along the beam propagation direction, the surface at the location where the fragmented particle resides is clearly fractured. The side towards the beam direction, on the other hand, shows optical features similar to those observed in Fig. 3b, which may result from a similar surface depression. These dramatic differences argue for further analysis of the response of the capping materials to the interaction between laser and particles of different shapes.

Fig. 5 shows the microscope images of selected sites on the Al_2O_3 capping layer after the single laser exposure at 10 J/cm^2. Fig. 5a is small region on the capping layer surface adopted from the optical microscope image shown in Fig. 4a which displays the marked features on the Al_2O_3 capping surface at the Ti particle location after single laser shot. At this resolution, it is difficult to discern the nature of the marked spots. To reveal the exact nature of these spots on the surface, high resolution SEM images were collected and their representatives marked by the circles are shown in Figs. 5b-d. These images clearly show that the dark regions seen in Fig. 5a are made of small Ti particles, fragmented from the parent Ti particle upon the laser shot. It is speculated that the recoil momentum from the ejected plasma causes the remnants of the heated particle to strike the capping layer surface and lead to fragmentation and that no damage occurs on the capping surface, even at the particle locations. The others locations show similar characteristics.

4. Phenomenology and Modeling

Laser light impinging on a metal can elevate its surface temperature through energy deposition within the optical skin depth. If the fluence is sufficiently high, the temperature can rise beyond the vaporization temperature. Subsequent interaction between the laser and vapor can cause further temperature elevation and result in plasma formation. In our earlier estimate [19], the fluence threshold for plasma formation was about 4.4 J/cm^2 for a 14 ns pulse. Thus under the present irradiation of 10 J/cm^2, plasma formation is expected. The plasma ejected from the Ti surface carries both thermal energy and momentum. Depending on the beam direction and the shape of the metal particle, the thermally-active plasma plume may intercept the surface on which the metallic particle resides which can lead to surface modification including plasm scalding [26]. In addition to transporting thermal energy, the plasma can also lead to recoil of the fragmented droplets and the remaining particle itself. The recoil momentum depends on the ejection direction of the plasma, which we will show to be strongly correlated to the shape of the particle. The shape dependence, in turn, leads to a marked difference in the response of the capping layer to the laser-particle interaction.

The combination of oblique incidence and reflective surfaces between the sphere and the substrate leads to an increased absorption on the Ti surface, as we have shown for a spherical particle [19]. The analysis utilized optical simulations with FRED. In short, for a spherical particle, the maximum absorbed intensity is shifted from 45 degrees above the equator to 10 degrees above the equator, as shown in Fig. 8 of [19]. In the presence of the mirror, the total power absorbed by the sphere is increased by 81%, and the maximum local absorbed intensity is increased by about 26% (shifted in location). Recall that the overall enhancement of absorption is increased by the mirror. Thus, in the presence of the reflective or mirror surface, it is sufficient

to have only 3.5 J/cm^2 instead of 4.4 J/cm^2 in the incident beam in order to generate plasma from the Ti particles.

The physical mechanisms of the plasma effects are illustrated in Fig. 6. The incident laser radiation absorbs into the metal, rapidly heating the surface and produces the initial plasma which is enhanced by the radiation reflected from the mirror. This increases the plasma generation which shifts the peak of intensity and plasma production downward toward the equator, as we noted. The hot plasma ejected as a result of rapid evaporation is partially deposited on the capping layer, resulting in heating and thermal expansion. While the thermal diffusivity of thin film is strongly dependent on deposition process, the trends between the two capping materials are thought to remain the same. The thermal diffusion time of the capping layer is estimated to be approximately ~ 10 μs which is much longer than that of the laser pulse width. The short duration of the interaction leaves the next layer cold, and the thermal expansion of the capping layer produces a delamination on the area affected by the plasma, which can be larger than the particle size (see Figs. 2 and 3). Since the thermal expansion coefficient of the Al_2O_3 much higher (by a factor of about 15) than that of fused silica, the delamination of the alumina layer is much more pronounced. However, if the capping layer is thicker than the thermal diffusion length during the plasma lifetime, delamination is suppressed and the mechanical strength of the material determines the extent of the damage. Further investigation is underway to explore the critical thickness of capping layer at which the delamination is suppressed.

The recoil momentum produced by the ejected plasma imparts motion to the particle, and the direction of the force is given by integration of the incident flux over the particle surface [27].

The partially melted particles move along the surface, sputtering small droplets and expanding the extent of damage.

In the case of a flattened particle, two modifying effects take place. First, as the oblateness increases, the reflected light couples less efficiently into the particle, and the region of peak intensity becomes smaller and moves toward the horizontal pole of the ellipsoid. As a result, less plasma is ejected, and it is directed increasingly toward the normal of the surface. Thus less plasma hits the substrate, and the thermally induced delamination diminishes. Second, with increasing oblateness, the recoil momentum becomes progressively more vertical. The vertical component of the recoil momentum presses the particles toward the substrate, increasing the mechanical energy coupling and decreasing the force causing motion along the surface.

To understand this behavior, FRED simulations were performed on Ti ellipsoids of successively increasing flatness. Five cases were considered: a spherical particle and 4 ellipsoids of aspect ratios (ratio of horizontal length to vertical length) 2:1, 4:1, 6:1, and 8:1. A sample absorption pattern on the 2:1 ellipsoid is shown in Fig. 7a. According to the calculations, the recoil angle with the horizontal increased from 7 degrees (for a spherical particle) to 77 degrees (for the 8:1 ellipsoid), as shown in Fig. 7b. Note that the slope decreases as the angle approaches vertical, as expected.

These simulation results also imply that for the irregular shaped Ti particle, the vertical component of the recoil momentum can be over 4 times larger than that with the spherical particle, potentially delivering a large mechanical impact onto the capping surface. The extent of modification or damage by laser-particle coupling on the capping layer thus will be directly related to the mechanical robustness of the capping material. Since the mechanical toughness of Al_2O_3 is 10 times larger than that of SiO_2, it is reasonable to hypothesize that the large disparity

in mechanical toughness is mainly responsible for the observed difference in response to laser-induced damage (see Fig. 4b) by the Ti particles of different shape. Furthermore, the strong mechanical toughness along with the large vertical recoil momentum is responsible for the fragmentation of the Ti filing on the Al_2O_3 capping layer, as displayed in Fig. 5.

Thus the large damage produced by spherical contaminants is greatly modified for oblate particles. We would note, parenthetically, that spherical particles have the weakest coupling with the surface and so can be most readily removed by cleaning procedures.

5. Conclusions

In summary, laser damage testing at oblique incidence shows that the laser-contaminant interaction on HR multilayer coatings leads to modification or damage to the surface protective capping layer. The damage behavior is strongly dependent on the shape of the contaminant particles and the composition of the capping material. For laser interaction with a spherical Ti particle, the damage is characterized by delamination of capping layers and can be related to the thermal properties of the capping materials. For laser interaction with irregularly-shaped particles, the damage is characterized by substrate fracture and can be related to the mechanical properties of the capping material. Specifically, in the presence of the spherical Ti contaminant, the Al_2O_3 capping layer shows much more severe damage than that of SiO_2, because Al_2O_3 has a thermal expansion coefficient that is 15 times larger than that of the SiO_2. On the other hand, in the presence of the Ti filings, the damage on the SiO_2 capping layer is more pronounced as the mechanical toughness of Al_2O_3 is 10 times larger than that of SiO_2. We have presented numerical simulations that demonstrate the dependence of the energy absorption and inferred laser-induced plasma orientation on particle shape. Overall, our results suggest that a material with a strong mechanical toughness, but a small thermal expansion coefficient, may be effective for use as a

capping material to protect against debris-induced laser ablation and damage on 1ω high power dielectric coating mirrors.

Acknowledgements

This work was performed under the auspices of the U.S. Department of Energy by Lawrence Livermore National Laboratory under Contract DE-AC52-07NA27344 and funded through Laboratory Directed Research and Development Grant 14-ERD-098. We would like to thank Gabe Guss, John Adams, and Raluca Negres for making fiducials, William G. Hollingsworth for performing the laser damage testing and optical microscope imaging, and Chantel Aracne-Ruddle for Ti filings separation.

References

[1] Stolz, C. J., "Status of NIF mirror technologies for completion of the NIF facility," Proc. of SPIE. 7101, 710115 (2008).

[2] Pinot, B., Leplan, H., Houbre, F. *et al.*, "Laser megajoule 1.06-μm mirror production with very high laser damage threshold," Proc. of SPIE. 4679, 234-241 (2002).

[3] Oliver, J. B., Rigatti, A. L., Howe, J. D. *et al.*, "Thin-film polarizers for the OMEGA EP laser system," Proc. of SPIE. 5991, 599119-1-8 (2005).

[4] Jitsuno, T., Murakami, H., Kato, K. *et al.*, "Recent progresses on insights of laser damage mechanisms and influence of contamination in optics," Proc. of SPIE. 8786, 87860B-6 (2013).

[5] Gourdin, W. H., Dzenitis, E. G., Martin, D. A. *et al.*, "Insitu surface debris inspection and removal system for upward-facing transport mirrors of the National Ignition Facility," Proc. of SPIE. 5647, 107-119 (2005).

[6] Ling, X. L., Wang, G., Zhao, Y. N. *et al.*, "Laser-induced damage of the optical coatings due to organic contamination in vacuum," Appl. Surf. Sci., 270, 346-351 (2013).

[7] Carniglia, C. K., Apfel, J. H., Allen, T. H. *et al.*, "Recent damage results on silica/titania reflectors at 1 micron," NBS Special Pub., 568, 377 (1979).

[8] Walton, C. C., Genin, F. Y., Chow, R. *et al.*, "Effect of silica overlayers on laser damage of HfO_2-SiO_2 56 degrees incidence high reflectors," Proc. of SPIE. 2714, 550-559 (1996).

[9] Wu, Z., Fan, Z., and Wang, Z., "Damage Threshold Dependence on Film Thickness," NIST Special Pub., 775, 321 (1988).

[10] Bajt, S., Edwards, N. V., and Madey, T. E., "Properties of ultrathin films appropriate for optics capping layers exposed to high energy photon irradiation," Surf. Sci. Rep., 63(2), 73-99 (2008).

[11] Wolfe, J. E., Qiu, S. R., and Stolz, C. J., "Fabrication of mitigation pits for improving laser damage resistance in dielectric mirrors by femtosecond laser machining," Appl. Opt., 50(9), C457-C462 (2011).

[12] Qiu, S. R., Wolfe, J. E., Monterrosa, A. M. *et al.*, "Searching for optimal mitigation geometries for laser-resistant multilayer high-reflector coatings," Appl. Opt., 50(9), C373-C381 (2011).

[13] Norton, M. A., Stolz, C. J., Donohue, E. E. *et al.*, "Impact of contaminates on the laser damage threshold of 1ω HR coatings," Proc. of SPIE. 5991, 59910O1-9 (2005).

[14] Stolz, C. J., Thomas, M. D., and Griffin, A. J., "BDS thin film damage competition," Proc. of SPIE. 7132, 71320C1-C7 (2008).

[15] Oliver, J. B., Kupinski, P., Rigatti, A. L. *et al.*, "Stress compensation in hafnia/silica optical coatings by inclusion of alumina layers," Opt. Express, 20(15), 16596-16610 (2012).

[16] Zhu, M., Yi, K., Li, D. *et al.*, "Study on the laser-induced damage performance of HfO_2, Sc_2O_3, Y_2O_3, Al_2O_3 and SiO_2 monolayer coatings," Proc. of SPIE. 8885, 8885081-8 (2013).

[17] Henyk, M., Wolfframm, D., and Reif, J., "Ultra short laser pulse induced charged particle emission from wide bandgap crystals," Appl. Surf. Sci., 168(1–4), 263-266 (2000).

[18] Reichling, M., Bodemann, A., and Kaiser, N., "Defect induced laser damage in oxide multilayer coatings for 248 nm," Thin Solid Films, 320(2), 264-279 (1998).

[19] Qiu, S. R., Norton, M. A., Raman, R. N. *et al.*, "Impact of laser-contaminant interaction on the performance of the protective capping layer of 1 omega high-reflection mirror coatings," Appl. Opt., 54(29), 8607-8616 (2015).

[20] Oliver, J. B., Howe, J., Rigatti, A. *et al.*, "High precision coating technology for large aperture NIF optics," Optical Interference Coatings, OSA Technical Digest (Optical Society of America, Washington, DC, ThD2 (2001).

[21] Anzellotti, J. F., Smith, D. J., Sczupak, R. J. *et al.*, "Stress and environmental shift characteristics of HfO_2/SiO_2 multilayer coatings,," Proc. of SPIE. 2966, 258-264 (1996).

[22] Boley, C. D., and Rubenchik, A. M., "Modeling of laser interactions with composite materials," Appl. Opt., 52(14), 3329-3337 (2013).
[23] Boley, C. D., Khairallah, S. A., and Rubenchik, A. M., "Calculation of laser absorption by metal powders in additive manufacturing," Appl. Opt., 54(9), 2477-2482 (2015).
[24] Matthews, M. J., Shen, N., Honig, J. *et al.*, "Phase modulation and morphological evolution associated with surface-bound particle ablation," Journal of the Optical Society of America B-Optical Physics, 30(12), 3233-3242 (2013).
[25] Harris, C. D., Shen, N., Rubenchik, A. M. *et al.*, "Characterization of laser-induced plasmas associated with energetic laser cleaning of metal particles on fused silica surfaces," Opt. Lett., 40(22), 5212-5215 (2015).
[26] Wang, H., Qi, H., Zhao, J. *et al.*, "Origin of the plasma scalds in dielectric coatings induced by 1ω laser," Appl. Phys. Lett., 108(14), 141603 (2016).
[27] Liedahl, D. A., Rubenchik, A., Libby, S. B. *et al.*, "Pulsed laser interactions with space debris: target shape effects," Advances in Space Research 52, (2013).

Figure Captions

Fig. 1 Morphology of representative surrogate Ti particles from (a) commercially available Ti spheres and (b) home-made Ti Filings. The Ti sphere shown has a diameter of 22 μm. The length of the Ti fillings shown is ~ 150 μm; its width ranges between 45-55 μm.

Fig. 2 Optical images of the Al_2O_3 capping layer surface: (a) with spherical Ti particle sprinkled on before laser shot and (b) after a single laser shot.

Fig. 3 Optical images of the SiO_2 capping layer surface: (a) with spherical Ti particle sprinkled on before laser shot and (b) after a single laser shot.

Fig. 4 Optical images of the capping layer surface after one laser shot at the presence of irregularly shaped Ti filings: (a) Al_2O_3 surface and (b) SiO_2 surface.

Fig. 5 Microscope images of particles on the Al_2O_3 capping surface after one laser shot at the presence of irregularly shaped Ti filings: (a) Optical image showing the surface features and (b) SEM images showing a closer view of the specific sites marked in (a). The sites are clearly from fragmented Ti particles and are not surface damage.

Fig. 6 Schematics showing the laser-induced plasma formation and particle recoil on reflective surface with (a) a spherical Ti particle, and (b) an oblate-shaped Ti particle.

Fig. 7 (a) Absorbed intensity on the surface of an ellipsoidal particle (aspect ratio 2:1) (b) Recoil angle versus aspect ratio.

Figure 1

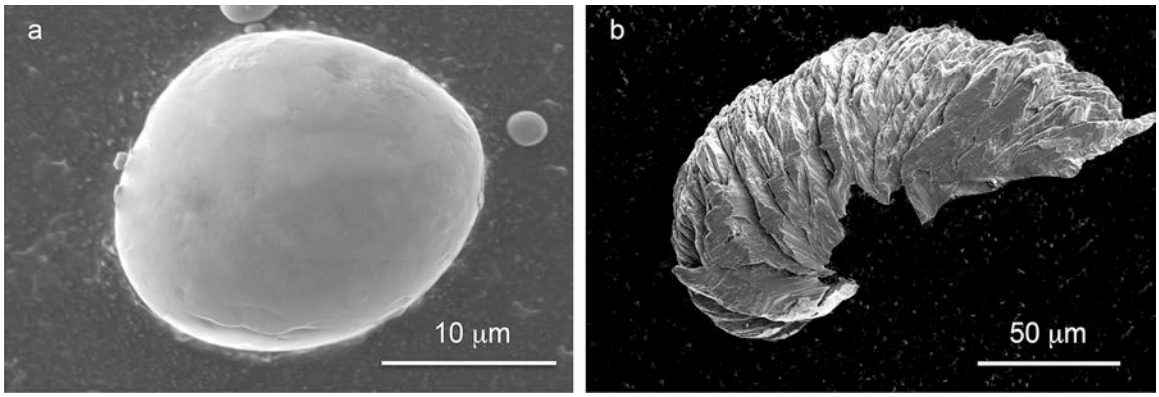

Figure 2

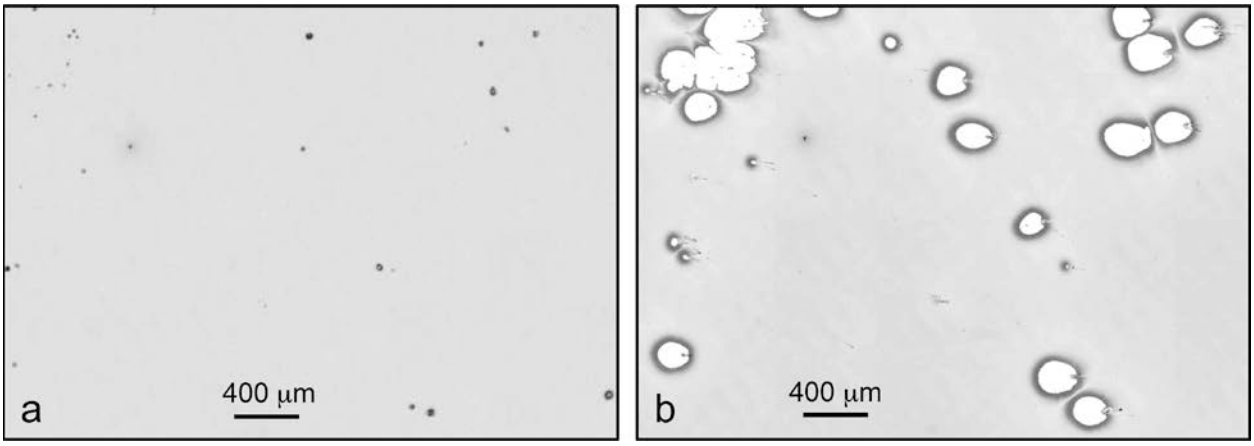

Figure 3

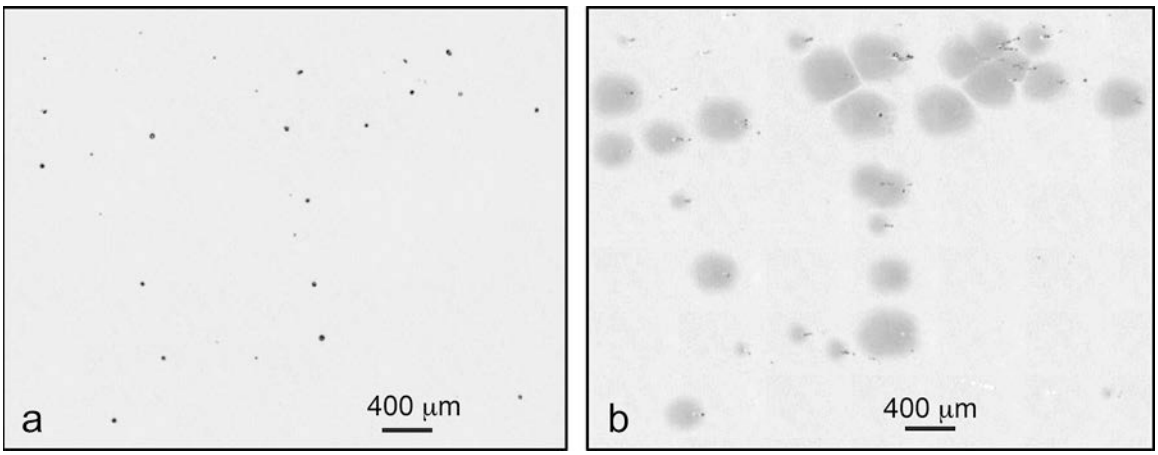

Figure 4

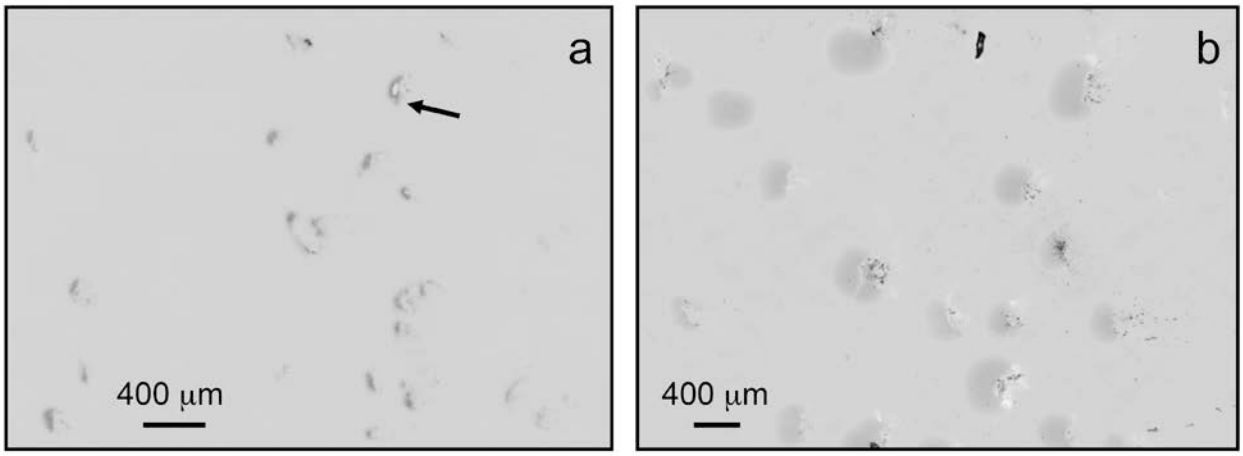

Figure 5

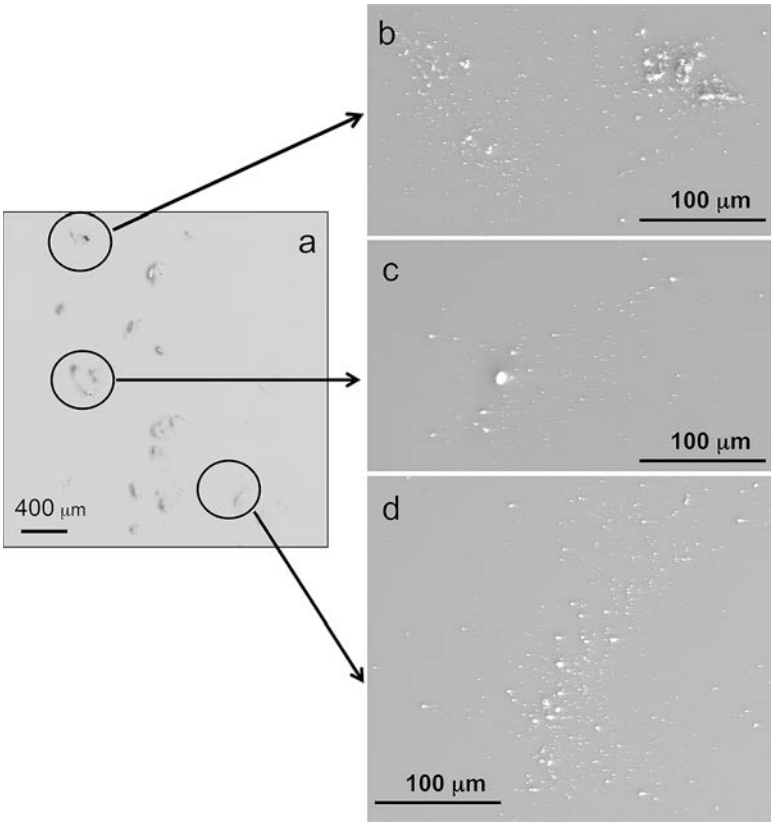

Figure 6

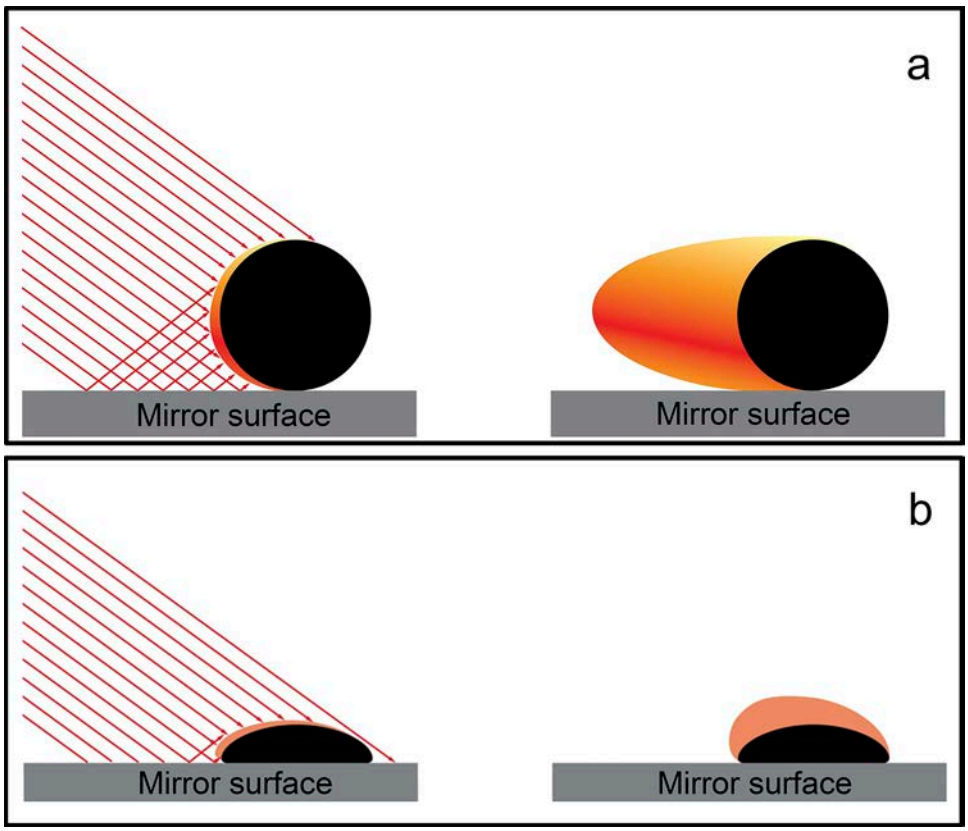
a
Mirror surface
Mirror surface
b
Mirror surface
Mirror surface

Figure 7